Cell

Rapid and Pervasive Changes in Genome-wide Enhancer Usage during Mammalian Development

Alex S. Nord,[1] Matthew J. Blow,[1,2] Catia Attanasio,[1] Jennifer A. Akiyama,[1] Amy Holt,[1] Roya Hosseini,[1] Sengthavy Phouanenavong,[1] Ingrid Plajzer-Frick,[1] Malak Shoukry,[1] Veena Afzal,[1] John L.R. Rubenstein,[3] Edward M. Rubin,[1,2] Len A. Pennacchio,[1,2,*] and Axel Visel[1,2,4,*]
[1]Genomics Division, MS 84-171, Lawrence Berkeley National Laboratory, Berkeley, CA 94720, USA
[2]U.S. Department of Energy Joint Genome Institute, Walnut Creek, CA 94598, USA
[3]Department of Psychiatry, Rock Hall, University of California, San Francisco, CA 94158-2324, USA
[4]School of Natural Sciences, University of California, Merced, CA 95343, USA
*Correspondence: lapennacchio@lbl.gov (L.A.P.), avisel@lbl.gov (A.V.)
http://dx.doi.org/10.1016/j.cell.2013.11.033

SUMMARY

Enhancers are distal regulatory elements that can activate tissue-specific gene expression and are abundant throughout mammalian genomes. Although substantial progress has been made toward genome-wide annotation of mammalian enhancers, their temporal activity patterns and global contributions in the context of developmental in vivo processes remain poorly explored. Here we used epigenomic profiling for H3K27ac, a mark of active enhancers, coupled to transgenic mouse assays to examine the genome-wide utilization of enhancers in three different mouse tissues across seven developmental stages. The majority of the ~90,000 enhancers identified exhibited tightly temporally restricted predicted activity windows and were associated with stage-specific biological functions and regulatory pathways in individual tissues. Comparative genomic analysis revealed that evolutionary conservation of enhancers decreases following midgestation across all tissues examined. The dynamic enhancer activities uncovered in this study illuminate rapid and pervasive temporal in vivo changes in enhancer usage that underlie processes central to development and disease.

INTRODUCTION

Distant-acting transcriptional enhancers represent the most abundant class of *cis*-regulatory sequences in mammalian genomes (Shen et al., 2012) and are predicted to be exceptionally tissue specific in function (Bernstein et al., 2012; Ernst et al., 2011; Shen et al., 2012; Visel et al., 2009). They are often associated with developmentally expressed genes (Levine, 2010) and can drive spatially highly restricted in vivo activity patterns (Pennacchio et al., 2006; Visel et al., 2009, 2013). Sequence-level changes at enhancers underlie evolutionary differences between species (Jones et al., 2012) and significantly contribute to the genetic etiology of human disease (Dickel et al., 2013; Bernstein et al., 2012; Ernst et al., 2011). As such, genome-wide maps of enhancers and their activity patterns provide insight into mechanisms of evolution, development, and disease, and significant progress has been made toward mapping these elements in mammalian genomes (Bernstein et al., 2012; Ernst et al., 2011; Shen et al., 2012). In parallel, in vivo transcriptome profiling of developing tissues has revealed highly dynamic gene expression during tissue ontogenesis (Bruneau, 2008; Kang et al., 2011; Si-Tayeb et al., 2010), and dysregulation of transient developmental gene-expression patterns has been linked to congenital defects and pathogenic traits (Garg et al., 2005; Hoerder-Suabedissen et al., 2013). Differences in the chromatin landscape between individual adult and embryonic tissues and in cultured cells (Gifford et al., 2013; Heintzman et al., 2009; Shen et al., 2012; Stergachis et al., 2013; Zhu et al., 2013; Ziller et al., 2013) raise the possibility that, within a given tissue, the genome-wide regulatory architecture might change substantially across developmental stages. Although these initial lines of evidence suggest that enhancers may play a significant role in the extensive changes in gene expression observed throughout mammalian development, the in vivo dynamics of enhancer utilization as individual tissues develop pre- and postnatally have been minimally explored. Profiling enhancer activity in developing tissues across a controlled time course has the potential to reveal the temporal dynamics of mammalian enhancer usage in vivo and capture regulatory landscapes orchestrating transient biological processes that are central to human health and disease.

RESULTS

Mapping Enhancer Activity Landscapes via H3K27ac Profiling of Mouse Tissues

To examine genome-wide enhancer activity at a consistent and defined temporal resolution, we performed epigenomic mapping of active enhancers across a developmental time series in three

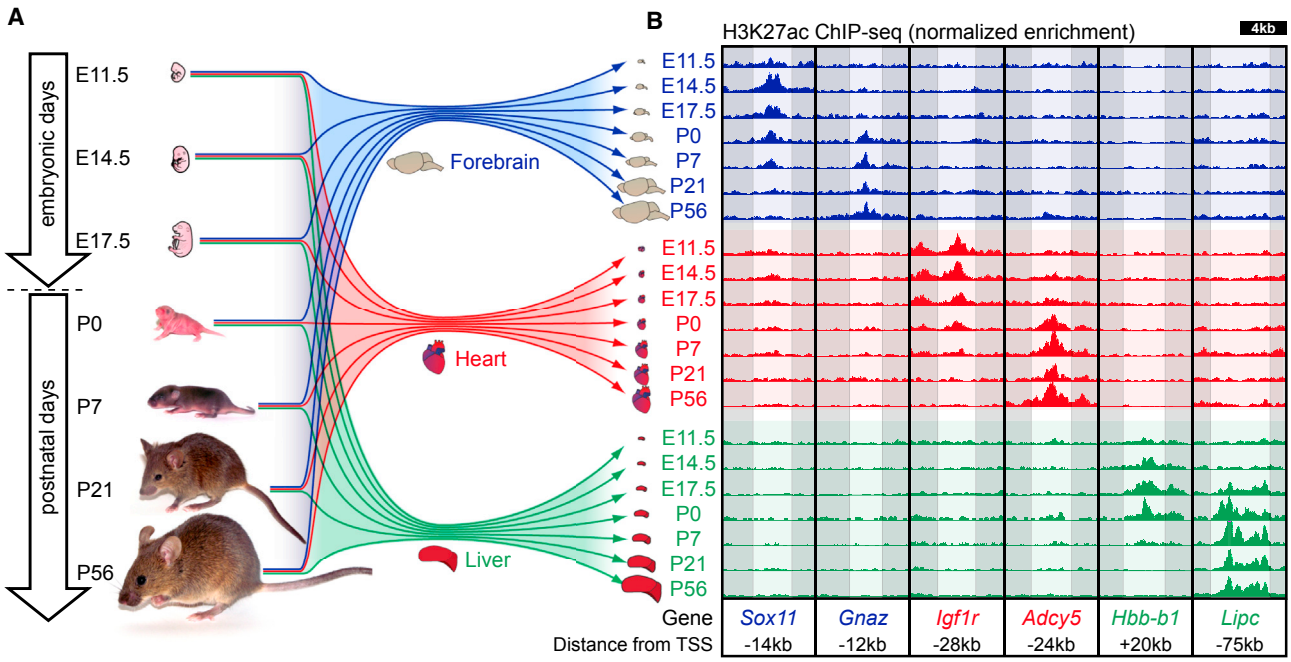

Figure 1. Mapping In Vivo Enhancers via ChIP-Seq Performed on Mouse Forebrain, Heart, and Liver Tissue

(A) Schematic of developmental stages and tissues.

(B) Representative examples of putative enhancers exhibiting dynamic H3K27ac signal across tissues and time points. Text includes description of loci.

See also Figures S1 and S2 and Table S1.

organs with different anatomical and physiological trajectories: forebrain, heart, and liver. The forebrain is the center of many higher brain functions, arising from the ectoderm and undergoing waves of neurogenesis and migration during mid-embryogenesis, with substantial late maturation (Austin and Cepko, 1990; Clinton et al., 2000; Kang et al., 2011). The heart arises from the mesoderm, is one of the earliest organs to form with basic patterning complete by late gestation, and performs the singular function of circulation throughout life (Brand, 2003; Harvey, 2002; Olson, 2006). The liver arises from the endoderm and goes through a major functional transition, switching from fetal hematopoiesis to its mature functions of detoxification, metabolism, and plasma protein and hormone synthesis late in gestation (Zhao and Duncan, 2005; Zorn, 2008). These three tissues are of significant relevance to biomedical research, and pathogenic traits associated with all three systems are closely linked to transient developmental processes.

We generated genome-wide maps of enhancers active in each of these organs via chromatin immunoprecipitation sequencing (ChIP-seq) performed directly on mouse tissue collected at different stages of development (Figure 1A). The developmental stages (embryonic days [E] 11.5, 14.5, and 17.5; postnatal days [P] 0, 7, 21, and 56) and tissues were selected to capture significant developmental processes in these major organ systems. In total, we profiled 21 unique tissue types collected from pre- and postnatal mice (Table S1 available online). We assessed the tissue- and stage-specific presence of H3K27ac, a histone modification found at active enhancers (Creyghton et al., 2010; Rada-Iglesias et al., 2011) and at transcription start sites (TSSs). Figure S1 shows a schematic overview of the analysis. ChIP-seq reads were mapped to mm9, and peaks were called for each data set (see Extended Experimental Procedures for details for all analyses). We separated the H3K27ac-enriched regions into putative distal enhancers, defined as regions positioned at least 1 kb from a known TSS, and proximal regions that were within 1 kb of or overlapped a TSS. In total, across the three tissues and seven time points examined, we identified 105,394 H3K27ac-enriched regions, including 16,225 regions that were proximal to known TSSs and 89,169 distal regions representing putative developmental enhancers. Comparison of expression levels of the nearest TSS for both forebrain and heart enhancers showed significantly increased expression in the linked tissue at E11.5 (t test p values: forebrain = 0.007; heart = 0.03). H3K27ac enrichment profiles for biological replicates for a subset of samples showed significant reproducibility across data sets (Figure S2A). The association of enhancers with gene expression, the biological reproducibility of ChIP-seq experiments, and patterns of H3K27ac coenrichment across tissues and time points support the validity of these data sets for genome-wide enhancer analysis (Figure S2).

Recent studies of chromatin indicate that H3K27ac is present at enhancers when they are active (Bonn et al., 2012; Cotney et al., 2012; Creyghton et al., 2010; Rada-Iglesias et al., 2011), suggesting a model wherein dynamic H3K27ac enrichment is associated with transient enhancer activity. This notion is illustrated by examples of differential H3K27ac enrichment across time points and tissues at representative putative distal enhancers located near selected developmentally active target

genes (Figure 1B). For instance, an enhancer with early forebrain H3K27ac enrichment was identified near *Sox11*, a gene critical for prenatal forebrain patterning (Bergsland et al., 2011; Shim et al., 2012; Uwanogho et al., 1995). In contrast, a region with postnatal H3K27ac enrichment in the forebrain was identified near *Gnaz*, a gene associated with dopamine signaling in the postnatal/adult forebrain (Hendry et al., 2000; Hinton et al., 1990; Leck et al., 2006; Sidhu et al., 1998). In the heart, two enhancers with early and late enrichment peaks were identified near *Igf1r* and *Adcy5*, consistent with known roles of these genes in early heart development and later cardiomyocyte survival, respectively (Donath et al., 1994; Holzenberger et al., 2000; Hu et al., 2009; Iwatsubo et al., 2004; Laustsen et al., 2007). Examples in the liver include a prenatal enhancer near *Hbb-b1*, which encodes a hemoglobin protein expressed in the embryonic liver during fetal hematopoiesis (Whitney, 1977), and *Lipc*, which encodes a hepatic lipase active in the mature liver that is implicated in cardiovascular disease in humans (Zambon et al., 2003). These examples suggest that dynamic chromatin modification is detectable at enhancers examined across developmental stages.

To investigate dynamic chromatin modification patterns genome-wide, the complete set of peaks called across all data sets was merged by combining peaks where the highest points of enrichment within individual peaks were within 1 kb. Each merged peak was then scored for enhancer activity across the 21 data sets based on H3K27ac signal strength. The results from this analysis show that time points next to each other and from the same tissue have the most similar H3K27ac enrichment profiles, as expected based on spatial and temporal relationships of the profiled tissues (Figure S2B). Initial clustering analysis indicated that developmental enhancers identified in this study largely exhibited restricted H3K27ac enrichment across tissues and temporally across developmental time points (Figure S2C). Using an enrichment classification method robust to false negatives in the ChIP-seq data, we predicted the activity windows of all enhancers identified in the three tissues. In comparison to shuffled data, predicted activity showed significant temporal and spatial correlation structure across time points and tissues, indicating that the patterns we observe represent real biological patterns.

Although differences in the genome-wide enhancer landscape between developing and mature tissues are known to exist in principle (May et al., 2012; Shen et al., 2012), this time-course profiling of an enhancer-specific chromatin mark enables longitudinal examination of predicted in vivo enhancer activities at high temporal resolution. In most cases (forebrain 85%; heart 66%; liver 80%), the predicted tissue-specific temporal activity window of putative enhancers spanned only a subset of the developmental stages examined (Figure 2A). The three tissues exhibit different patterns with regard to predicted enhancer activity across stages that are in line with their respective developmental trajectories (Figures 2A–2D and S2). For example, a larger proportion of putative heart enhancers exhibit constitutive predicted activity, consistent with the embryonic heart already attaining many aspects of its mature function at E11.5, the earliest time point profiled. Putative distal enhancers map to both intergenic (42%) and intragenic (58%) chromosomal regions, where they overlap with intronic sequence (41%), coding exons (9%), and untranslated regions (8%) (Figure 2B). In addition to temporal activity restrictions, candidate enhancers were predicted to be predominantly tissue specific (Figure 2C), with 42,976 (48%) expected to be active only in one of the three tissues examined. Illustrating the rapidly changing enhancer landscape, 40,696 (45%) of putative distal enhancers identified here are predicted to have highly restricted temporal activity, with enrichment spanning at most two consecutive time points in a given tissue (Figure 2D). Although many enhancers that exhibit short activity windows are tissue specific, we also identified clusters of enhancers with predicted activity across multiple tissues (Figure S2) that may control general or shared developmental and/or functional processes. Considering only the ~3% of putative enhancers that showed constitutive H3K27ac enrichment across all tissues and time points, we observe strong enrichment near genes associated with hematological traits, suggesting that such enhancers are active in blood lineages present in all tissue samples. In contrast to the dynamic epigenomic landscape of enhancers, H3K27ac enrichment at TSSs does not exhibit such tissue- or stage-specific patterns, with 74% of TSSs exhibiting enrichment across all three tissues and the majority of TSS-proximal sites exhibiting constitutive enrichment within a tissue across all time points (forebrain 75%; heart 79%; liver 73%) (Figures 2B and S2). Overall, these results suggest that the genome-wide enhancer landscape active in each of the three organs undergoes extensive and fast-paced turnover during development.

In Vivo Validation of Enhancer Activity Predictions

The genome-wide changes in H3K27ac enrichment across stages support the prevalence of dynamic enhancer activity based on a known epigenomic signature of active enhancers. To obtain direct evidence of developmentally dynamic enhancer activities, we used an established transgenic mouse enhancer reporter assay (Kothary et al., 1989; Pennacchio et al., 2006) to experimentally validate enhancer activity predictions (Figure 3). Whole-mount staining of the transgenic mice generated in this assay is possible at E11.5 and E14.5, enabling interrogation of higher numbers of candidate enhancers at these early developmental stages compared to later time points, when sectioning is required. As such, we used three strategies to validate H3K27ac-based activity predictions using these assays. First, to establish baseline success rates for in vivo activity predictions made from H3K27ac data sets, we examined sequences predicted to be active forebrain enhancers at E11.5, where 12/18 (67%) drove reproducible expression patterns in vivo (Figures 3A and S3). This rate of validated in vivo activity is similar to that of other epigenomic marks of active enhancers, such as p300 (Visel et al., 2009), and is significantly higher than the rate of in vivo forebrain enhancer activity among a control set of tested highly conserved noncoding presumed functional elements (Pennacchio et al., 2006) (Fisher's exact test, $p = 6 \times 10^{-6}$). Next, we examined in vivo activity of a smaller set of eight enhancers at multiple time points to validate that change in H3K27ac enrichment corresponded to changes in in vivo activity. We examined sequences that were known to be inactive in vivo at E11.5 (Pennacchio et al., 2006) but exhibited an H3K27ac enrichment profile

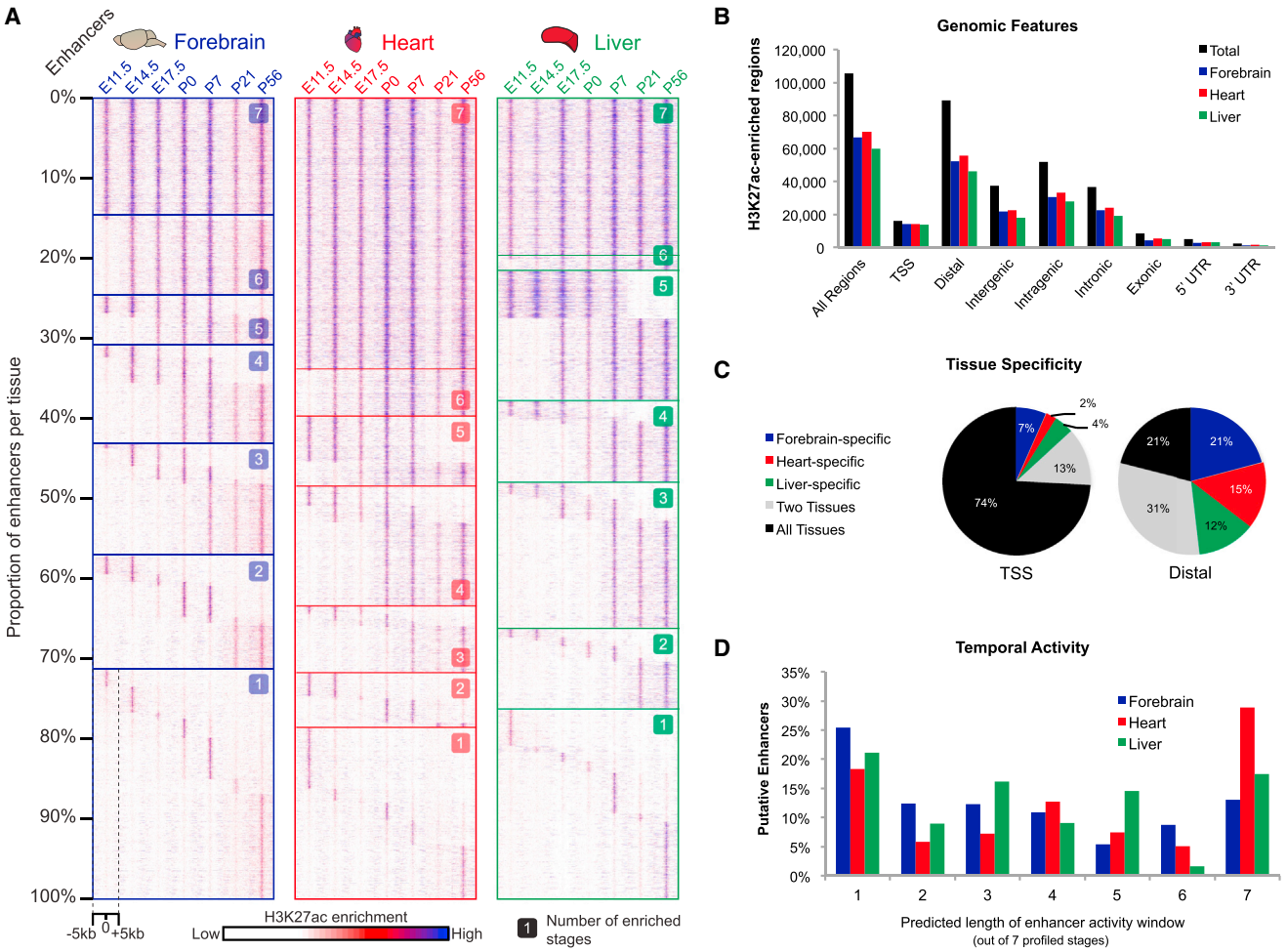

Figure 2. Developmental Enhancers Exhibit Dynamic H3K27ac Enrichment Associated with In Vivo Activity

(A) Heatmap displaying H3K27ac enrichment by tissue and time point for putative distal enhancers (forebrain, n = 52,175; heart, n = 55,869; liver, n = 46,062). For each tissue, each row of the heatmap shows relative H3K27ac enrichment at one enhancer, with signal across the surrounding 10 kb region plotted. Enhancers are organized by the number of time points at which the enhancer is active, starting with constitutively active enhancers at the top and proceeding down to single-stage enhancers at the bottom.

(B) Breakdown on H3K27ac enrichment across genomic features.

(C) Tissue specificity for TSS and distal H3K27ac enrichment.

(D) Predicted length of putative distal enhancer activity based on H3K27ac enrichment across seven profiled time points.

See also Figure S2.

that suggested activity at later time points. 5/8 (63%) of the elements tested showed reproducible in vivo forebrain activity at a later time point consistent with the developmental H3K27ac signature (Figure S4). We additionally re-examined two elements where activity was predicted to subside later in development and that were active in E11.5. In one of the two, we observed no reproducible LacZ staining at E17.5 or P0. Representative staining patterns for two dynamic enhancers are shown in Figures 3B and 3C. First, an enhancer near *Scn2a1*, a sodium channel gene expressed in the forebrain between E11.5 and E14.5 (Albrieux et al., 2004) that is required for normal brain development (Planells-Cases et al., 2000) and mutated in autism (Sanders et al., 2012), showed highly reproducible cortical expression at E11.5 but not at P0 (Figure 3B). Second, an enhancer near *Elavl2*, a gene important to neuronal differentiation (Akamatsu et al., 1999), had no activity at E11.5 but drove reproducible expression in the hippocampus at P0 (Figure 3C). Finally, we tested six enhancers where the human orthologous region overlapped a lead genome-wide association study (GWAS) single-nucleotide polymorphism (SNP) associated with a forebrain, heart, or liver phenotype. The lead SNPs overlapped by the tested enhancers were not in linkage disequilibrium with a coding SNP, and lead SNPs overlapped with putative transcription factor (TF)-binding motifs predicted using HaploReg (Ward and Kellis, 2012). All six candidate enhancers drove expression in the predicted tissue at E14.5 (Figure S5). Three representative enhancers that overlap GWAS lead SNPs are shown in Figure 3D, including an enhancer active in the fetal mouse liver that contains

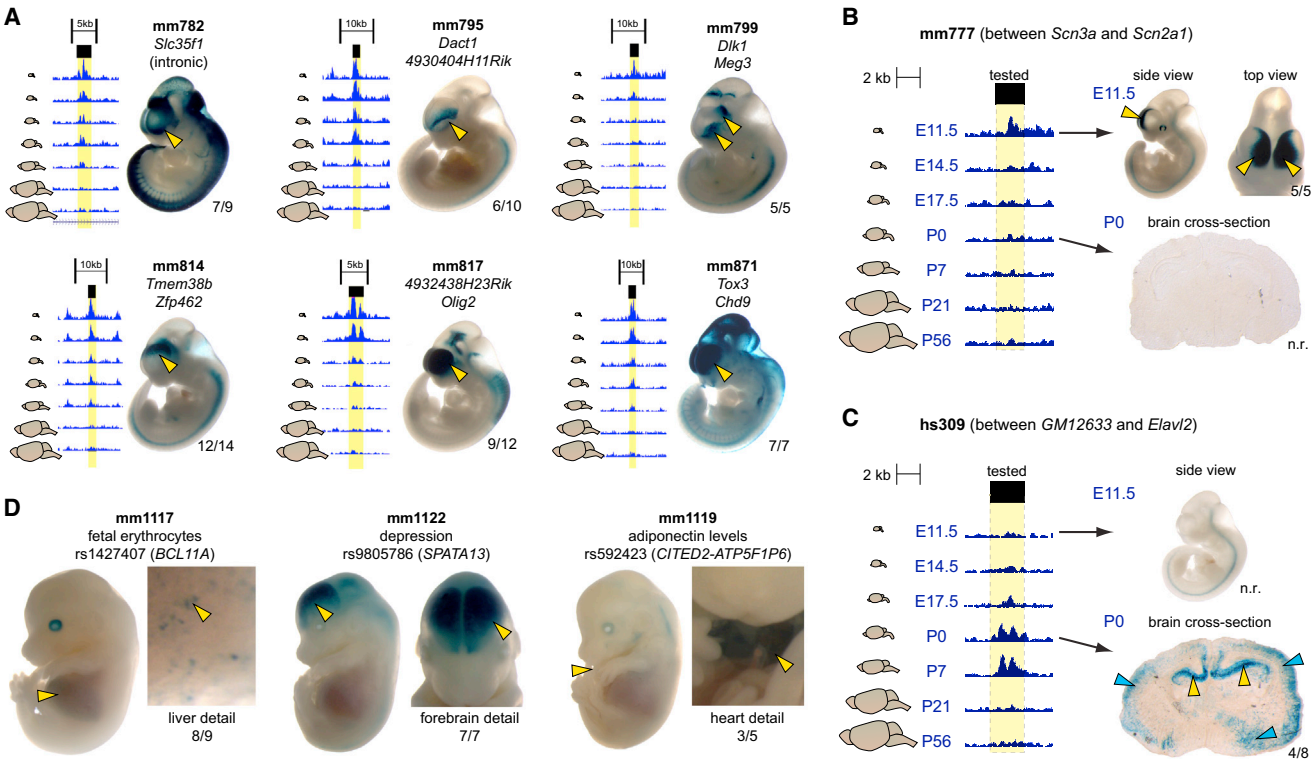

Figure 3. In Vivo Validation of H3K27ac-Predicted Enhancer Activity

Candidate enhancers were cloned into a vector containing a minimal promoter and the LacZ reporter gene and injected into fertilized mouse oocytes. Multiple transgenic mice with independent enhancer integration events were examined to assess the reproducibility of any given reporter activity pattern. Yellow arrows and numbers next to embryos/sections indicate reproducibility of staining across transgenic individuals. Additional embryo images for each element can be viewed in the VISTA Enhancer Database (http://enhancer.lbl.gov). n.r., not reproducible.

(A–C) In vivo validation of predicted forebrain enhancers. Forebrain H3K27ac signal across time points shown to the left, with yellow highlighting indicating the tested region. (A) Six representative enhancers that exhibit diverse forebrain activity patterns at E11.5. (B) Enhancer located near *Scn2a1* that shows transient H3K27ac enrichment and drives in vivo expression at E11.5, but not P0. (C) Enhancer upstream of *Elavl2* that shows transient enrichment and in vivo activity at P0, but not E11.5. Blue arrows indicate nonreproducible staining.

(D) Three representative enhancers active at E14.5 that overlap with lead GWAS SNPs. For mm1119, reproducible staining was also present in liver, consistent with H3K27ac enrichment in E14.5 liver (not shown). GWAS phenotype, lead SNP ID, and potential gene of interest are listed.

See also Figures S3, S4, and S5.

a SNP associated with levels of blood cells with fetal hemoglobin (F-cells) in adults (Bhatnagar et al., 2011; Menzel et al., 2007), an enhancer that is active in the developing mouse forebrain that contains a lead SNP for depression and alcohol dependence (Edwards et al., 2012), and a mouse heart and liver enhancer that contains a SNP associated with adiponectin levels (Dastani et al., 2012). These experimentally validated enhancer activity patterns provide in vivo evidence suggesting plausible pathogenic mechanisms of noncoding variation via spatiotemporally restricted impact on target gene expression caused by changes in enhancer sequence. In total, 23/32 (72%) putative enhancers tested in transgenic mice drove H3K27ac-predicted expression patterns in vivo, and many of these enhancers were associated with critical developmental genes or potentially pathogenic variation. Full transgenic results from all experiments performed for this study are available on the VISTA website (http://enhancer.lbl.gov/). Together, the genome-wide ChIP-seq data and the complementary transgenic validation of a subset of dynamic activity predictions support the existence of very large numbers of enhancers with restricted activity intervals across development.

Enhancers Control Dynamic Developmental Processes and Are Enriched for TF-Binding Motifs and Disease-Associated Variation

To assess correlation between the predicted temporal activity of enhancers and biological function beyond anecdotal examples, we examined on a genome-wide scale whether putative enhancers can be linked to biological processes, mouse phenotypes, and regulatory pathways associated with the developmental stages profiled (Heinz et al., 2010; McLean et al., 2010). Putative enhancers are globally enriched near genes that have pertinent tissue- and time point-related functional annotations and are enriched for relevant TF-binding sites. For example, enhancers predicted to be active early in forebrain development are enriched for annotation terms such as *neural precursor cell*

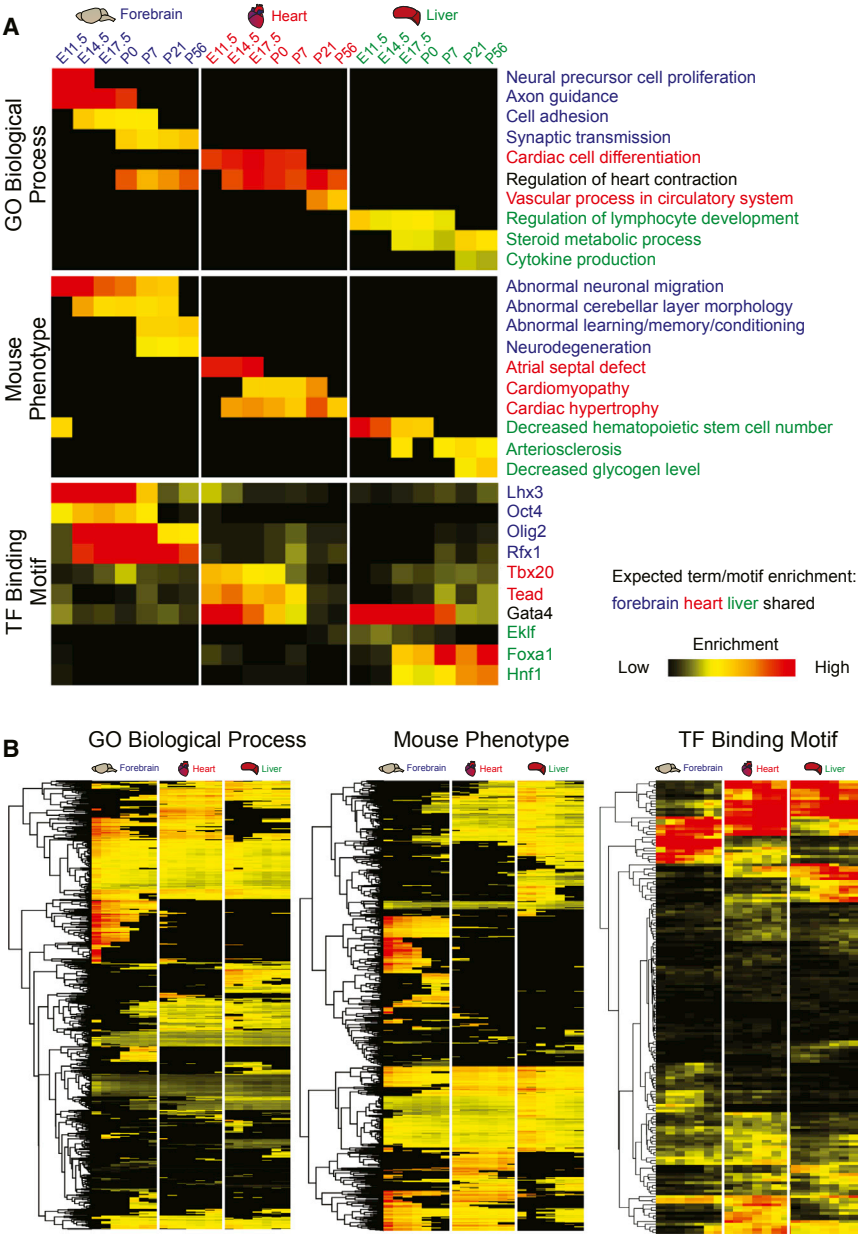

Figure 4. Association of Developmental Enhancers with Functional Pathways, Mouse Phenotypes, and TF-Binding Motifs

Each heatmap displays results from enrichment analysis performed on forebrain, heart, and liver enhancers active at specified time points.

(A) Ten representative differentially enriched GO biological functions, MGI mouse phenotypes, and known TF-binding motifs selected from the complete enrichment data sets.

(B) Full enrichment data set heatmaps for GO biological functions (n = 827), MGI mouse phenotypes (n = 922), and known TF-binding motifs (n = 215). Annotation terms and TF motifs were hierarchically clustered by enrichment patterns. Differential enrichment across tissues and time points occurs widely across the full data sets.

proliferation and *axonogenesis* and binding motifs of TFs that control neuronal differentiation, such as *Lhx3*. In contrast, enhancers predicted to be active later in forebrain development are enriched for biological processes such as *synaptic transmission* and *cognition* and phenotypes including *abnormal learning/memory/conditioning* and *neurodegeneration*. Figure 4A shows ten representative functions, phenotypes, and binding motifs that exhibit strong differential enrichment patterns across tissues and developmental stages, with such differential patterns recapitulated across the entire set of enriched annotation terms and binding motifs, as shown in Figure 4B. Finally, intersection of putative enhancers identified here with results from genome-wide association studies (Hindorff et al., 2009) showed that disease-associated SNPs are more likely to be located nearby candidate enhancers compared to randomly sampled SNPs (see Extended Experimental Procedures). These results demonstrate that transiently active developmental enhancers are centrally involved in the control of biological processes required for tissue ontogenesis and function, regulating genes essential to developmental and disease phenotypes.

Evolutionary Pressure on Enhancers Changes across Development

Despite the general utility of evolutionary conservation as a mark of regulatory sequences (Pennacchio and Rubin, 2001), studies in mammalian cell lines and tissues have produced contradictory findings regarding the global conservation levels of enhancers (Blow et al., 2010; Bernstein et al., 2012; Pennacchio et al., 2006; Shen et al., 2012). The maps of predicted enhancer activity in the present study, obtained with consistent methodology across tissues and developmental stages, provide an opportunity to examine the evolutionary conservation of enhancers using rigorous comparative genomic measurements. To test whether evolutionary pressure on enhancers varies across tissues or developmental stages, the most constrained core regions of noncoding putative distal enhancers active at different developmental stages were compared using two related measures of sequence evolution, conservation (evolutionary age based on divergence between mouse and most distant vertebrate lineage exhibiting sequence homology to mouse) and constraint (estimate of local sequence conservation across vertebrates). In addition to tissue-derived data, we incorporated in this analysis H3K27ac ChIP-seq data from mouse embryonic stem cells (ESCs) and three cell lineages, neural progenitors, mesoderm, and mesoendoderm,

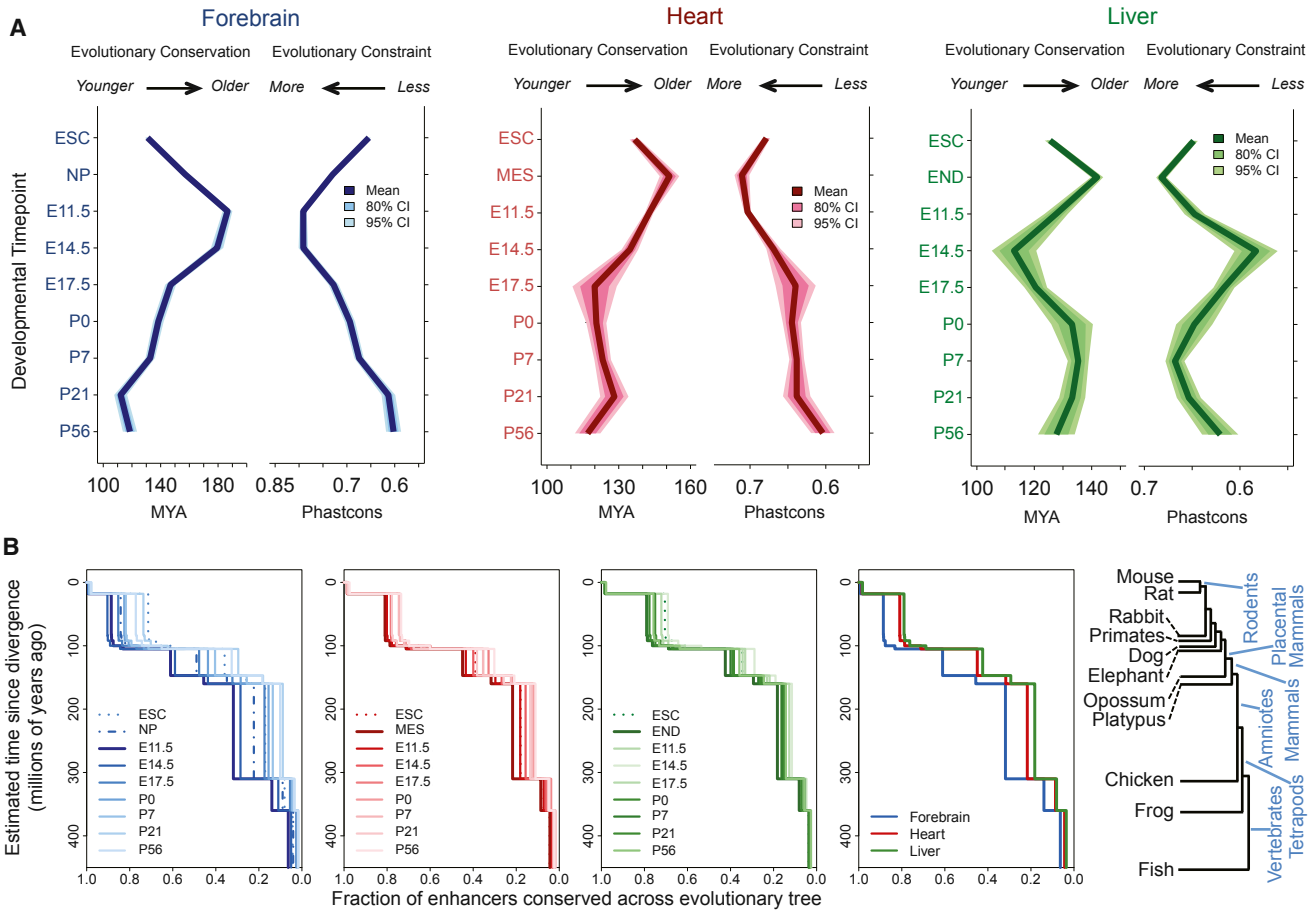

Figure 5. Developmental Signatures of Enhancer Evolution

The tissue-based enhancer set was expanded to include cell lines used as proxies for early development: embryonic stem cells (ESC), neural progenitors (NP), mesoderm (MES), and mesoendoderm (END).

(A) Mean and 95% and 80% confidence intervals of evolutionary age (left panel) and constraint (right panel) by tissue and time point.

(B) Cumulative proportion of enhancers conserved across the vertebrate tree (shown on right) as defined by enhancer sequence homology. Plots shown for all time points in each individual tissue in the first three panels, with higher mean conservation indicated by darker shades. Far-right panel shows differences across tissues at the most constrained stage for each tissue.

See also Figures S6 and S7.

as experimentally accessible proxies for major lineages of the forebrain, heart, and liver at stages prior to E11.5.

Strikingly, we observed substantial differences in evolutionary conservation and sequence constraint of putative enhancers compared both within a given tissue across time points and across tissues at the same time point (Figure 5A). Predicted forebrain enhancers exhibit higher overall constraint and are more conserved across the vertebrate tree than enhancers predicted to be active in heart or liver, verifying previous findings comparing enhancers active at E11.5 identified by p300 binding (Blow et al., 2010). However, for all tissues, the maximum levels of evolutionary conservation/constraint of putative enhancers were observed in early embryogenesis, with a second phase of temporarily increased conservation/constraint in the liver in early postnatal development. These differences result in distinct tissue-specific evolutionary signatures of in vivo enhancers across development that were robustly reproduced using alternative constraint metrics, phylogenetic comparisons, and expected enhancer core sizes (Figure S6).

To examine the evolutionary history of enhancers, the cumulative percent of enhancers conserved across each transition was determined using sequence homology across the 100 most constrained bases, plotted in Figure 4B. The color of plotted lines correlates with the summary measures for the data set (shown in Figure 4A), with darker color tones indicating stronger overall constraint/conservation. We reasoned that if specific evolutionary transitions disproportionally contributed to the overall differences in conservation observed across tissues and time points, the effect would be reflected by large differences between stages/tissues at specific transitions across the vertebrate tree. For example, the transition to a fully septated heart, present through chicken but not in frogs or more distant vertebrates (Olson, 2006), might be associated with a significantly lower proportion of enhancers conserved across the

transition from tetrapods to amniotes relative to the transition from amniotes to placental mammals. Across accessible evolutionary divergence events, the relative proportions of conserved enhancers recapitulated the general patterns observed for mean conservation and constraint (Figure 5B). At least at the level of whole-organ development, these results suggest that the observed tissue- and stage-specific differences represent cumulative effects of increased selective pressure on enhancers active early in embryonic development throughout more than 400 million years of vertebrate evolution.

We observed two further relationships with enhancer constraint: positive correlation between constraint and distance from the nearest TSS and a TSS distance-independent effect where intergenic enhancers exhibited increased constraint versus intronic enhancers (Figure S7). These patterns are manifested by a larger proportion of enhancers with predicted activity in mature tissues located nearby the TSS and within gene bodies relative to the same tissues at earlier stages, a pattern that is partially consistent with recent findings comparing adult tissues to differentiating cell lineages (Zhu et al., 2013). The strength of these patterns varied across tissues, with forebrain exhibiting increases in the difference in distance to the nearest TSS and proportion of intronic enhancers between time points relative to the other two tissues. These patterns indicate that constraint and position in the genome are interconnected with regard to stage of enhancer activity and suggest that these patterns may be driven by general aspects of genome evolution and structure.

DISCUSSION

We report the developmental activity annotation of nearly 90,000 candidate distal enhancers across three major mammalian organ systems. These genome-wide enhancer activity profiles obtained directly from ex vivo tissues across multiple stages of the mammalian lifespan provide insight into the temporal utilization of enhancers as it occurs in vivo in the developing organism. Mapping dynamic H3K27ac enrichment alone is a basic model for enhancer identification and activity prediction, as H3K27ac is unlikely to be present at all active enhancers, may not correlate universally with enhancer activity, and may be present at other noncoding genomic features. In the future, concurrent analysis of additional informative chromatin marks and genome-wide binding or transcription data sets is likely to refine enhancer activity maps further, enabling increased sensitivity and specificity with regard to enhancer activity predictions and a corresponding increase in the success rate of in vivo validation assays. These limitations notwithstanding, the strong global signatures of dynamic predicted enhancer activity in our results coupled with transgenic validation of in vivo activity predictions demonstrate the power of interrogating relevant tissues across developmental transitions. Most of the candidate enhancers identified here are predicted to have tightly restricted temporal activity windows, indicating that dynamic processes in mammalian development and tissue ontogenesis are regulated by the transient activities of large numbers of temporally and spatially restricted developmental enhancers. The rapid temporal changes in enhancer landscape identified via time-course profiling mirror patterns of dynamic gene expression across development, suggesting that regulatory control of spatiotemporal gene-expression patterns is accomplished through the combinatorial activity of regulatory elements that far outnumber coding genes. These findings have major ramifications in the context of predicting regulatory elements controlling clinically relevant tissue- and stage-specific processes and regarding efforts to systematically map enhancers in the human genome. While validating the importance and impact of large-scale efforts to annotate functional genomic elements, our observations also highlight a substantial challenge in producing a complete functional annotation of all distant-acting enhancers in the human genome. The large numbers of putative enhancers identified here with predicted short activity windows in specific tissues suggest that tightly spaced developmental time series from diverse panels of tissues may be required to capture a truly comprehensive picture of the genome-wide enhancer landscape.

The observation of very high constraint of enhancers predicted to be active at mid-gestation corroborates and partially explains reports that as many as half of all extremely conserved noncoding sequences may act as enhancers in vivo at E11.5, with particular enrichment for neuronal tissue activities (Pennacchio et al., 2006; Visel et al., 2008). These findings are in line with recent whole-embryo transcriptome studies of zebrafish and *Drosophila* and with evolutionary signatures observed at regulatory sequences across human cell lineages that support the evolutionary hourglass model of development (Domazet-Lošo and Tautz, 2010; Kalinka et al., 2010; Stergachis et al., 2013). This model posits that increased evolutionary constraint at critical stages of embryogenesis produces high levels of similarity across evolutionary lineages during early development, with relaxed constraint and increased evolutionary divergence before and after these critical stages (Raff, 1996). The results from this study show that distinct patterns of sequence evolution apply to enhancers with transient in vivo activities in mammalian development and identify tissue-specific variation in the timing and level of maximum constraint that suggest differences in the evolutionary history of different organ systems. The tissue-specific differences in the timing of maximal enhancer constraint coincide with transitional phases during the ontogenesis of these three organs. Enhancer constraint in the developing forebrain peaks at E11.5 and continues to be high at E14.5, spanning critical stages of forebrain patterning and neuronal migration (Austin and Cepko, 1990). In contrast, maximal constraint in the heart is observed at E11.5, consistent with early maturation of the heart during embryogenesis (Harvey, 2002), and average enhancer constraint is relatively stable from E17.5 through P56. In liver, a similar early maximum in enhancer constraint is present, with a secondary peak around P7, which tracks the transition from fetal hematopoiesis to the assumption of the predominantly metabolic functions of the mature liver (Zorn, 2008). Although these explanations are speculative, it is clear that evolutionary pressure on enhancers changes in a tissue-specific manner across development. These dynamic evolutionary signatures of active enhancers reconcile previous contradicting findings regarding constraint of mammalian enhancers, illuminate evolutionary forces shaping development, and reinforce the long-held notion that regulatory DNA is a primary substrate upon which evolution acts (King and Wilson, 1975).

EXPERIMENTAL PROCEDURES

The Extended Experimental Procedures contain detailed methods and references for all analyses described in the text and below. All custom analysis scripts are available from the authors at request.

ChIP-Seq

Tissues from pre- and postnatal CD-1 mice were collected on ice, crosslinked using formaldehyde, and lysed with SDS-based reagents, and chromatin was sonicated on a Diagenode Bioruptor instrument using ChIP-seq protocols optimized for mouse tissues (Visel et al., 2009). Chromatin immunoprecepitation (ChIP) was performed using antibodies for H3K27ac (Abcam Ab4729). Prepared libraries from ChIP and input DNA were sequenced on an Illumina HiSeq instrument. For all experiments, reads were mapped to mm9 using BWA (Li and Durbin, 2009), and peaks were called using MACS (Zhang et al., 2008).

Enhancer Activity Prediction and In Vivo Validation

Using the merged set of H3K27ac peaks, enrichment for each region in each data set was scored based on comparison of coverage within the candidate enhancer versus experiment background after input correction. Enrichment scores across experiments were analyzed using both unsupervised and supervised approaches to determine the tissue- and stage-specific activity profiles for each putative enhancer. Activity predictions were validated using an established mouse transgenic system (Kothary et al., 1989; Pennacchio et al., 2006), where a vector containing a candidate enhancer, a minimal promoter, and the LacZ gene are stably integrated into the mouse genome via standard pronuclear injection. An enhancer was considered validated if the LacZ staining pattern driven by the enhancer in F0 transgenic mice was consistent with the H3K27ac predicted activity across independent transgenic mice representing independent insertion events in the mouse genome.

Functional and Evolutionary Analysis

Functional annotation of putative enhancers was performed with the GREAT tool (McLean et al., 2010), which tests for global enhancer enrichment near annotated gene classes. Motif analysis was performed with the HOMER tool (Heinz et al., 2010). Overlap with GWAS SNPs (Hindorff et al., 2009) was compared to overlap with non-GWAS SNPs present on standard genotyping arrays, and individual candidate enhancers harboring GWAS SNPs were selected for validation of enhancer activity via the transgenic assay. Evolutionary analysis included six additional cell-derived H3K27ac ChIP-seq data sets that were processed using the same methods. Base-wise sequence homology and evolutionary constraint were compared for the core enhancer region (defined as the 100 bp within the enhancer regions exhibiting maximal constraint) across accessible vertebrate genomes. Additional details are reported in the Extended Experimental Procedures.

Access to Full Data Sets

Complete data files are available online at http://enhancer.lbl.gov/mouse_timecourse and include enhancer predictions mapped to the mouse reference genome (mm9) in BED and TXT format, predicted enhancer coordinates lifted over to the human reference genome (hg19), overlap between predicted enhancers and lead GWAS SNPs, and results from functional annotation and motif enrichment analyses as text files and labeled heatmaps.

ACCESSION NUMBERS

H3K27ac ChIP-seq data from this study are available in GEO (http://www.ncbi.nlm.nih.gov/geo/) under accession number GSE52386.

SUPPLEMENTAL INFORMATION

Supplemental Information includes Extended Experimental Procedures, seven figures, and one table and can be found with this article online at http://dx.doi.org/10.1016/j.cell.2013.11.033.

ACKNOWLEDGMENTS

The authors thank Chia-lin Wei and Cindy Choi for help with chromatin immunoprecipitation from embryonic mouse tissue and Diane Dickel and Han Wu for guidance and advice regarding enhancer activity analysis. A.S.N. was supported by NIH/NIGMS NRSA F32 fellowship GM105202. C.A. was supported by a SNSF advanced researchers fellowship. A.V. and L.A.P. were supported by NIH grants R01NS062859A, R01HG003988, and U01DE020060. J.L.R.R. was supported by NIMH grant R37MH049428. Research was conducted at the E.O. Lawrence Berkeley National Laboratory and performed under Department of Energy Contract DE-AC02-05CH11231, University of California.

Received: October 1, 2013
Revised: October 28, 2013
Accepted: November 22, 2013
Published: December 19, 2013

REFERENCES

Akamatsu, W., Okano, H.J., Osumi, N., Inoue, T., Nakamura, S., Sakakibara, S., Miura, M., Matsuo, N., Darnell, R.B., and Okano, H. (1999). Mammalian ELAV-like neuronal RNA-binding proteins HuB and HuC promote neuronal development in both the central and the peripheral nervous systems. Proc. Natl. Acad. Sci. USA *96*, 9885–9890.

Albrieux, M., Platel, J.-C., Dupuis, A., Villaz, M., and Moody, W.J. (2004). Early expression of sodium channel transcripts and sodium current by cajal-retzius cells in the preplate of the embryonic mouse neocortex. J. Neurosci. *24*, 1719–1725.

Austin, C.P., and Cepko, C.L. (1990). Cellular migration patterns in the developing mouse cerebral cortex. Development *110*, 713–732.

Bergsland, M., Ramsköld, D., Zaouter, C., Klum, S., Sandberg, R., and Muhr, J. (2011). Sequentially acting Sox transcription factors in neural lineage development. Genes Dev. *25*, 2453–2464.

Bernstein, B.E., Birney, E., Dunham, I., Green, E.D., Gunter, C., and Snyder, M.; ENCODE Project Consortium (2012). An integrated encyclopedia of DNA elements in the human genome. Nature *489*, 57–74.

Bhatnagar, P., Purvis, S., Barron-Casella, E., DeBaun, M.R., Casella, J.F., Arking, D.E., and Keefer, J.R. (2011). Genome-wide association study identifies genetic variants influencing F-cell levels in sickle-cell patients. J. Hum. Genet. *56*, 316–323.

Blow, M.J., McCulley, D.J., Li, Z., Zhang, T., Akiyama, J.A., Holt, A., Plajzer-Frick, I., Shoukry, M., Wright, C., Chen, F., et al. (2010). ChIP-Seq identification of weakly conserved heart enhancers. Nat. Genet. *42*, 806–810.

Bonn, S., Zinzen, R.P., Girardot, C., Gustafson, E.H., Perez-Gonzalez, A., Delhomme, N., Ghavi-Helm, Y., Wilczyński, B., Riddell, A., and Furlong, E.E.M. (2012). Tissue-specific analysis of chromatin state identifies temporal signatures of enhancer activity during embryonic development. Nat. Genet. *44*, 148–156.

Brand, T. (2003). Heart development: molecular insights into cardiac specification and early morphogenesis. Dev. Biol. *258*, 1–19.

Bruneau, B.G. (2008). The developmental genetics of congenital heart disease. Nature *451*, 943–948.

Clinton, M., Manson, J., McBride, D., and Miele, G. (2000). Gene expression changes during murine postnatal brain development. Genome Biol. *1*, RESEARCH0005.

Cotney, J., Leng, J., Oh, S., DeMare, L.E., Reilly, S.K., Gerstein, M.B., and Noonan, J.P. (2012). Chromatin state signatures associated with tissue-specific gene expression and enhancer activity in the embryonic limb. Genome Res. *22*, 1069–1080.

Creyghton, M.P., Cheng, A.W., Welstead, G.G., Kooistra, T., Carey, B.W., Steine, E.J., Hanna, J., Lodato, M.A., Frampton, G.M., Sharp, P.A., et al. (2010). Histone H3K27ac separates active from poised enhancers and predicts developmental state. Proc. Natl. Acad. Sci. USA *107*, 21931–21936.

Dastani, Z., Hivert, M.-F., Timpson, N., Perry, J.R.B., Yuan, X., Scott, R.A., Henneman, P., Heid, I.M., Kizer, J.R., Lyytikäinen, L.-P., et al.; DIAGRAM+ Consortium; MAGIC Consortium; GLGC Investigators; MuTHER Consortium; DIAGRAM Consortium; GIANT Consortium; Global B Pgen Consortium; Procardis Consortium; MAGIC investigators; GLGC Consortium (2012). Novel loci for adiponectin levels and their influence on type 2 diabetes and metabolic traits: a multi-ethnic meta-analysis of 45,891 individuals. PLoS Genet. *8*, e1002607.

Dickel, D.E., Visel, A., and Pennacchio, L.A. (2013). Functional anatomy of distant-acting mammalian enhancers. Philos. Trans. R. Soc. Lond. B Biol. Sci. *368*, 20120359.

Domazet-Lošo, T., and Tautz, D. (2010). A phylogenetically based transcriptome age index mirrors ontogenetic divergence patterns. Nature *468*, 815–818.

Donath, M.Y., Zapf, J., Eppenberger-Eberhardt, M., Froesch, E.R., and Eppenberger, H.M. (1994). Insulin-like growth factor I stimulates myofibril development and decreases smooth muscle alpha-actin of adult cardiomyocytes. Proc. Natl. Acad. Sci. USA *91*, 1686–1690.

Edwards, A.C., Aliev, F., Bierut, L.J., Bucholz, K.K., Edenberg, H., Hesselbrock, V., Kramer, J., Kuperman, S., Nurnberger, J.I., Jr., Schuckit, M.A., et al. (2012). Genome-wide association study of comorbid depressive syndrome and alcohol dependence. Psychiatr. Genet. *22*, 31–41.

Ernst, J., Kheradpour, P., Mikkelsen, T.S., Shoresh, N., Ward, L.D., Epstein, C.B., Zhang, X., Wang, L., Issner, R., Coyne, M., et al. (2011). Mapping and analysis of chromatin state dynamics in nine human cell types. Nature *473*, 43–49.

Garg, V., Muth, A.N., Ransom, J.F., Schluterman, M.K., Barnes, R., King, I.N., Grossfeld, P.D., and Srivastava, D. (2005). Mutations in NOTCH1 cause aortic valve disease. Nature *437*, 270–274.

Gifford, C.A., Ziller, M.J., Gu, H., Trapnell, C., Donaghey, J., Tsankov, A., Shalek, A.K., Kelley, D.R., Shishkin, A.A., Issner, R., et al. (2013). Transcriptional and epigenetic dynamics during specification of human embryonic stem cells. Cell *153*, 1149–1163.

Harvey, R.P. (2002). Patterning the vertebrate heart. Nat. Rev. Genet. *3*, 544–556.

Heintzman, N.D., Hon, G.C., Hawkins, R.D., Kheradpour, P., Stark, A., Harp, L.F., Ye, Z., Lee, L.K., Stuart, R.K., Ching, C.W., et al. (2009). Histone modifications at human enhancers reflect global cell-type-specific gene expression. Nature *459*, 108–112.

Heinz, S., Benner, C., Spann, N., Bertolino, E., Lin, Y.C., Laslo, P., Cheng, J.X., Murre, C., Singh, H., and Glass, C.K. (2010). Simple combinations of lineage-determining transcription factors prime cis-regulatory elements required for macrophage and B cell identities. Mol. Cell *38*, 576–589.

Hendry, I.A., Kelleher, K.L., Bartlett, S.E., Leck, K.J., Reynolds, A.J., Heydon, K., Mellick, A., Megirian, D., and Matthaei, K.I. (2000). Hypertolerance to morphine in G(z alpha)-deficient mice. Brain Res. *870*, 10–19.

Hindorff, L.A., Sethupathy, P., Junkins, H.A., Ramos, E.M., Mehta, J.P., Collins, F.S., and Manolio, T.A. (2009). Potential etiologic and functional implications of genome-wide association loci for human diseases and traits. Proc. Natl. Acad. Sci. USA *106*, 9362–9367.

Hinton, D.R., Blanks, J.C., Fong, H.K., Casey, P.J., Hildebrandt, E., and Simons, M.I. (1990). Novel localization of a G protein, Gz-alpha, in neurons of brain and retina. J. Neurosci. *10*, 2763–2770.

Hoerder-Suabedissen, A., Oeschger, F.M., Krishnan, M.L., Belgard, T.G., Wang, W.Z., Lee, S., Webber, C., Petretto, E., Edwards, A.D., and Molnár, Z. (2013). Expression profiling of mouse subplate reveals a dynamic gene network and disease association with autism and schizophrenia. Proc. Natl. Acad. Sci. USA *110*, 3555–3560.

Holzenberger, M., Leneuve, P., Hamard, G., Ducos, B., Perin, L., Binoux, M., and Le Bouc, Y. (2000). A targeted partial invalidation of the insulin-like growth factor I receptor gene in mice causes a postnatal growth deficit. Endocrinology *141*, 2557–2566.

Hu, C.-L., Chandra, R., Ge, H., Pain, J., Yan, L., Babu, G., Depre, C., Iwatsubo, K., Ishikawa, Y., Sadoshima, J., et al. (2009). Adenylyl cyclase type 5 protein expression during cardiac development and stress. Am. J. Physiol. Heart Circ. Physiol. *297*, H1776–H1782.

Iwatsubo, K., Minamisawa, S., Tsunematsu, T., Nakagome, M., Toya, Y., Tomlinson, J.E., Umemura, S., Scarborough, R.M., Levy, D.E., and Ishikawa, Y. (2004). Direct inhibition of type 5 adenylyl cyclase prevents myocardial apoptosis without functional deterioration. J. Biol. Chem. *279*, 40938–40945.

Jones, F.C., Grabherr, M.G., Chan, Y.F., Russell, P., Mauceli, E., Johnson, J., Swofford, R., Pirun, M., Zody, M.C., White, S., et al.; Broad Institute Genome Sequencing Platform & Whole Genome Assembly Team (2012). The genomic basis of adaptive evolution in threespine sticklebacks. Nature *484*, 55–61.

Kalinka, A.T., Varga, K.M., Gerrard, D.T., Preibisch, S., Corcoran, D.L., Jarrells, J., Ohler, U., Bergman, C.M., and Tomancak, P. (2010). Gene expression divergence recapitulates the developmental hourglass model. Nature *468*, 811–814.

Kang, H.J., Kawasawa, Y.I., Cheng, F., Zhu, Y., Xu, X., Li, M., Sousa, A.M.M., Pletikos, M., Meyer, K.A., Sedmak, G., et al. (2011). Spatio-temporal transcriptome of the human brain. Nature *478*, 483–489.

King, M.C., and Wilson, A.C. (1975). Evolution at two levels in humans and chimpanzees. Science *188*, 107–116.

Kothary, R., Clapoff, S., Darling, S., Perry, M.D., Moran, L.A., and Rossant, J. (1989). Inducible expression of an hsp68-lacZ hybrid gene in transgenic mice. Development *105*, 707–714.

Laustsen, P.G., Russell, S.J., Cui, L., Entingh-Pearsall, A., Holzenberger, M., Liao, R., and Kahn, C.R. (2007). Essential role of insulin and insulin-like growth factor 1 receptor signaling in cardiac development and function. Mol. Cell. Biol. *27*, 1649–1664.

Leck, K.J., Blaha, C.D., Matthaei, K.I., Forster, G.L., Holgate, J., and Hendry, I.A. (2006). Gz proteins are functionally coupled to dopamine D2-like receptors in vivo. Neuropharmacology *51*, 597–605.

Levine, M. (2010). Transcriptional enhancers in animal development and evolution. Curr. Biol. *20*, R754–R763.

Li, H., and Durbin, R. (2009). Fast and accurate short read alignment with Burrows-Wheeler transform. Bioinformatics *25*, 1754–1760.

May, D., Blow, M.J., Kaplan, T., McCulley, D.J., Jensen, B.C., Akiyama, J.A., Holt, A., Plajzer-Frick, I., Shoukry, M., Wright, C., et al. (2012). Large-scale discovery of enhancers from human heart tissue. Nat. Genet. *44*, 89–93.

McLean, C.Y., Bristor, D., Hiller, M., Clarke, S.L., Schaar, B.T., Lowe, C.B., Wenger, A.M., and Bejerano, G. (2010). GREAT improves functional interpretation of cis-regulatory regions. Nat. Biotechnol. *28*, 495–501.

Menzel, S., Garner, C., Gut, I., Matsuda, F., Yamaguchi, M., Heath, S., Foglio, M., Zelenika, D., Boland, A., Rooks, H., et al. (2007). A QTL influencing F cell production maps to a gene encoding a zinc-finger protein on chromosome 2p15. Nat. Genet. *39*, 1197–1199.

Olson, E.N. (2006). Gene regulatory networks in the evolution and development of the heart. Science *313*, 1922–1927.

Pennacchio, L.A., and Rubin, E.M. (2001). Genomic strategies to identify mammalian regulatory sequences. Nat. Rev. Genet. *2*, 100–109.

Pennacchio, L.A., Ahituv, N., Moses, A.M., Prabhakar, S., Nobrega, M.A., Shoukry, M., Minovitsky, S., Dubchak, I., Holt, A., Lewis, K.D., et al. (2006). In vivo enhancer analysis of human conserved non-coding sequences. Nature *444*, 499–502.

Planells-Cases, R., Caprini, M., Zhang, J., Rockenstein, E.M., Rivera, R.R., Murre, C., Masliah, E., and Montal, M. (2000). Neuronal death and perinatal lethality in voltage-gated sodium channel alpha(II)-deficient mice. Biophys. J. *78*, 2878–2891.

Rada-Iglesias, A., Bajpai, R., Swigut, T., Brugmann, S.A., Flynn, R.A., and Wysocka, J. (2011). A unique chromatin signature uncovers early developmental enhancers in humans. Nature *470*, 279–283.

Raff, R.A. (1996). The Shape of Life: Genes, Development, and the Evolution of Animal Form (Chicago, IL: University of Chicago Press).

Sanders, S.J., Murtha, M.T., Gupta, A.R., Murdoch, J.D., Raubeson, M.J., Willsey, A.J., Ercan-Sencicek, A.G., DiLullo, N.M., Parikshak, N.N., Stein, J.L., et al. (2012). De novo mutations revealed by whole-exome sequencing are strongly associated with autism. Nature *485*, 237–241.

Shen, Y., Yue, F., McCleary, D.F., Ye, Z., Edsall, L., Kuan, S., Wagner, U., Dixon, J., Lee, L., Lobanenkov, V.V., and Ren, B. (2012). A map of the cis-regulatory sequences in the mouse genome. Nature *488*, 116–120.

Shim, S., Kwan, K.Y., Li, M., Lefebvre, V., and Sestan, N. (2012). Cis-regulatory control of corticospinal system development and evolution. Nature *486*, 74–79.

Si-Tayeb, K., Lemaigre, F.P., and Duncan, S.A. (2010). Organogenesis and development of the liver. Dev. Cell *18*, 175–189.

Sidhu, A., Kimura, K., Uh, M., White, B.H., and Patel, S. (1998). Multiple coupling of human D5 dopamine receptors to guanine nucleotide binding proteins Gs and Gz. J. Neurochem. *70*, 2459–2467.

Stergachis, A.B., Neph, S., Reynolds, A., Humbert, R., Miller, B., Paige, S.L., Vernot, B., Cheng, J.B., Thurman, R.E., Sandstrom, R., et al. (2013). Developmental fate and cellular maturity encoded in human regulatory DNA landscapes. Cell *154*, 888–903.

Uwanogho, D., Rex, M., Cartwright, E.J., Pearl, G., Healy, C., Scotting, P.J., and Sharpe, P.T. (1995). Embryonic expression of the chicken Sox2, Sox3 and Sox11 genes suggests an interactive role in neuronal development. Mech. Dev. *49*, 23–36.

Visel, A., Prabhakar, S., Akiyama, J.A., Shoukry, M., Lewis, K.D., Holt, A., Plajzer-Frick, I., Afzal, V., Rubin, E.M., and Pennacchio, L.A. (2008). Ultraconservation identifies a small subset of extremely constrained developmental enhancers. Nat. Genet. *40*, 158–160.

Visel, A., Blow, M.J., Li, Z., Zhang, T., Akiyama, J.A., Holt, A., Plajzer-Frick, I., Shoukry, M., Wright, C., Chen, F., et al. (2009). ChIP-seq accurately predicts tissue-specific activity of enhancers. Nature *457*, 854–858.

Visel, A., Taher, L., Girgis, H., May, D., Golonzhka, O., Hoch, R.V., McKinsey, G.L., Pattabiraman, K., Silberberg, S.N., Blow, M.J., et al. (2013). A high-resolution enhancer atlas of the developing telencephalon. Cell *152*, 895–908.

Ward, L.D., and Kellis, M. (2012). HaploReg: a resource for exploring chromatin states, conservation, and regulatory motif alterations within sets of genetically linked variants. Nucleic Acids Res. *40* (Database issue), D930–D934.

Whitney, J.B., 3rd. (1977). Differential control of the synthesis of two hemoglobin beta chains in normal mice. Cell *12*, 863–871.

Zambon, A., Deeb, S.S., Pauletto, P., Crepaldi, G., and Brunzell, J.D. (2003). Hepatic lipase: a marker for cardiovascular disease risk and response to therapy. Curr. Opin. Lipidol. *14*, 179–189.

Zhang, Y., Liu, T., Meyer, C.A., Eeckhoute, J., Johnson, D.S., Bernstein, B.E., Nusbaum, C., Myers, R.M., Brown, M., Li, W., and Liu, X.S. (2008). Model-based analysis of ChIP-Seq (MACS). Genome Biol. *9*, R137.

Zhao, R., and Duncan, S.A. (2005). Embryonic development of the liver. Hepatology *41*, 956–967.

Zhu, J., Adli, M., Zou, J.Y., Verstappen, G., Coyne, M., Zhang, X., Durham, T., Miri, M., Deshpande, V., De Jager, P.L., et al. (2013). Genome-wide chromatin state transitions associated with developmental and environmental cues. Cell *152*, 642–654.

Ziller, M.J., Gu, H., Müller, F., Donaghey, J., Tsai, L.T.-Y., Kohlbacher, O., De Jager, P.L., Rosen, E.D., Bennett, D.A., Bernstein, B.E., et al. (2013). Charting a dynamic DNA methylation landscape of the human genome. Nature *500*, 477–481.

Zorn, A.M. (2008). Liver Development (Cambridge, MA: Harvard Stem Cell Institute).